Effect of ground fault hazards on continuous pipelines: an approximate design framework

Pengpeng Ni, Ian D. Moore & W. Andy Take
GeoEngineering Centre at Queen's – RMC, Department of Civil Engineering – Queen's University, Kingston, ON K7L 3N6, Canada

ABSTRACT
Permanent ground displacements induced by seismic faulting can damage buried pipelines due to the complex combinations of bending moment and axial compression or tension that develop. In this paper, a pipeline interacting with a normal fault having a dip angle of 90° has been investigated using 3D finite element modeling. The pipe is characterized using hexahedron continuum elements surrounded by soil modeled as a standard Mohr-Coulomb material. The soil-pipeline interface is represented using the contact surface approach, which allows finite sliding and separation between the two surfaces. After evaluating the performance of the analysis against the centrifuge tests conducted by Saiyar (2011), a parametric analysis is carried out to extend the database for a range of relative pipe-soil stiffnesses. In beam-on-spring analysis, it is difficult to choose spring stiffness and correctly impose ground motion for this kind of analysis. Other existing analytical methods require iterative procedures to calculate the pipe strains, approaches that are difficult to use in practice. An approximate design framework is therefore proposed based on both the centrifuge and numerical results to evaluate the peak pipe curvature. This can be used as a first approximation for design, which eliminates the errors associated with the selection of soil springs during design, and the complexity of other analytical approaches.

RÉSUMÉ
Les déplacements permanents de sol induits par des failles sismiques peuvent endommager les canalisations enterrées en raison des combinaisons complexes de moment de flexion et à la compression axiale ou de tension qui se développent. Dans cet article, un pipeline qui interagie avec une faille normale ayant un angle d'inclinaison de 90 ° a été étudiée en utilisant la modélisation 3D par éléments finis. Le tuyau est caractérisé en utilisant des éléments du continuum d'hexaèdre environnant par le sol modélisé comme un matériau de Mohr-Coulomb standard. L'interface entre le sol et pipeline est représenté en utilisant l'approche de la surface de contact, ce qui permet de glissement finie, et la séparation entre les deux surfaces. Après l'évaluation de la performance d'analyse par rapport aux essais de centrifugation conduits par Saiyar (2011), une analyse paramétrique a été réalisée pour étendre la base de données pour une série de rigidités relatives au pipe-sol. Dans l'analyse de faisceau en ressort, il est difficile de choisir la raideur du ressort et correctement imposer le mouvement du sol pour ce type d'analyse. D'autres méthodes d'analyse existantes nécessitent des procédures itératives pour calculer la fatigue dans les pipe, les approches qui sont difficiles à utiliser en pratique. Un cadre de conception approximative est donc proposé sur la base à la fois sur la centrifugeuse et des résultats numériques pour évaluer la courbure de la conduite de pointe. Ceci peut être utilisé comme une première approximation pour la conception, ce qui élimine les erreurs associées à la sélection des ressorts de sol lors de la conception et de la complexité d'autres approches analytiques.

1 INTRODUCTION

After earthquakes, pipeline networks can be disrupted: (a) ruptures in gas lines and electricity lines induce fire; (b) breaks in water lines inhibit the control of fires; (c) leakage of oil and sewage pipelines leads to environmental and other impacts. It is generally recognized that permanent ground movements produce higher pipeline damage than transient seismic wave propagation (O'Rourke and Liu 1999). Surface faulting, landslides, seismic settlement and lateral spread due to soil liquefaction are all sources of permanent ground deformation. This paper examines pipeline response subject to normal faulting (Figure 1).

In this scenario, a pipeline is buried within a uniform soil layer above the base rock stratum. The burial depth H and bedding depth BD are defined as the distance from the centreline of the pipe to the ground surface and the base rock respectively. A normal fault is examined in the base rock, with the soil block remaining stationary on the footwall side and experiencing downward movement (δ_0) on the hanging wall side. Both the dip angle and the fault-pipeline intersecting angle are 90°. If there is no buried pipe, the fault introduces displacement discontinuities within the soil medium, which propagate up through the soil layer and eventually reach the ground surface. The evolution of this band of shearing soil can be altered by the pipe, where it bridges across from the footwall to the hanging wall side, and gaps may develop between pipe and soil. These complex soil-pipe interactions are often tackled using beam-on-spring analysis (ASCE 1984). However, the selection of soil spring stiffness is challenging. Other existing analytical solutions (Karamitros et al. 2007; 2011; Kennedy et al. 1977; Newmark and Hall 1975; Trifonov and Cherniy 2010; Wang and Yeh 1985) all feature very complex iterations, which hinder their application in practice. When pipes are designed for areas prone to differential ground motion,

structural engineers need the maximum bending moment to be evaluated. A method that is efficient to use and straightforward to understand is required.

Centrifuge tests on normal fault-pipeline interaction have been performed by Ha et al. (2008), Saiyar (2011) and Saiyar et al. (2011). In the earlier work by the authors, three-dimensional finite element analyses have been calibrated against Saiyar's centrifuge experiments (Ni et al. 2014). Both the free field soil response and pipe flexural responses were well reproduced. The analysis is therefore used to conduct a short parametric study to investigate the nature of normal fault-pipeline interaction when the relative pipe-soil stiffness varies. Finally, an approximate design framework is being developed to serve as a first level screening of design parameters.

2 CENTRIFUGE TESTS

Large scale experiments involving infrastructure like pipelines are difficult and costly when conducted in the laboratory. Reduced-scale model tests may be conducted at 1 g to examine behaviour, but the reliability of such tests is doubtful since the soil stress at comparable points at prototype scale are not replicated. As an alternative, centrifuge testing is attractive since increased gravity helps to produce stress fields within the reduced-scale model that are identical or close to those in the prototype (Schofield 1980; Taylor 2004). Reduced-scale tests are

also easier to control and more affordable than full-scale experiments.

Saiyar (2011) performed a series of centrifuge tests at 30 g using the beam centrifuge at C-CORE, to study the soil-structure interaction for pipelines crossing normal faults with dip angle of 90°. The normal fault rupture through the soil layer was produced by applying a dislocation to the translating floor of the test box, thereby representing the fault offset in a rock stratum as shown in Figure 2. In this paper, all results are presented in the centrifuge-based scale, unless otherwise stated.

Solid rods with length of 800 mm and diameter of 9.525 mm were fabricated in accordance to generate flexural stiffness equivalent to that of the prototype pipes. Pipe ends were not anchored. For example, a solid Aluminum rod was used as a small-scale model of a cast iron pipe having diameter of 285 mm and wall thickness of 10 mm. Other pipe properties and the relative pipe-soil stiffness are summarized in Table 1. All tests were controlled to have a maximum fault offset around 7 mm (0.21 m in the prototype) to load the pipe in the elastic range. This facilitates use of thin beam theory to derive the flexural responses of the pipe.

The soil used in the tests was Fraser River sand. This is a uniform material with d_{50} = 0.26 mm (Wijewickreme et al. 2005). Dry pluviation was employed to get a target soil density of 1610 kg/m^3 corresponding to a relative density of 80%.
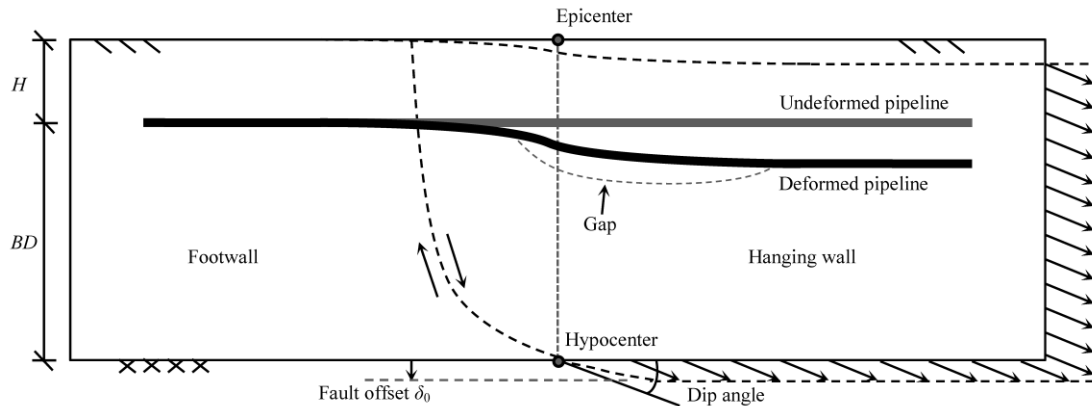
Figure 1. Definition and geometry of the problem
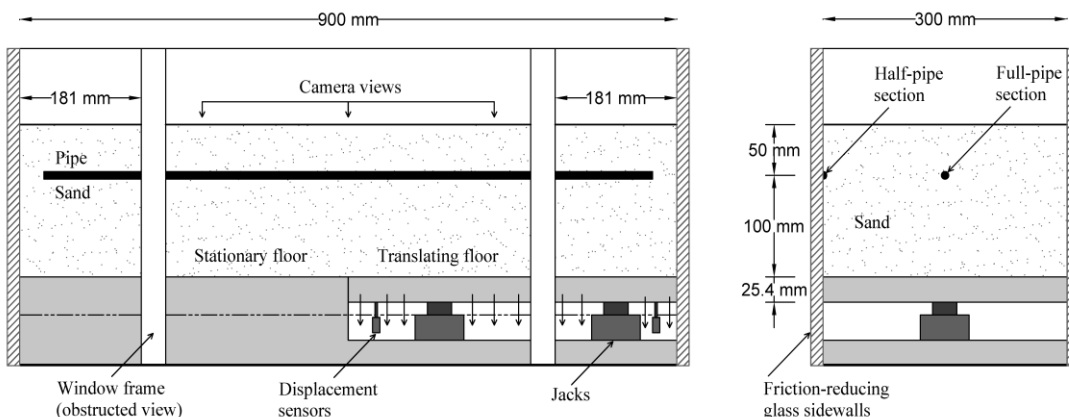
Figure 2. Centrifuge test geometry (from Saiyar et al. 2011)

Table 1. Properties of model pipes in the centrifuge test and the finite element study.

Pipe Material	Pipe1[*]	Teflon	Pipe2[*]	Polycarbonate	Acrylic	Pipe3[*]	Pipe4[*]	Aluminum
E_p (MPa)	150	420	1000	2200	3200	10000	30000	69000
E_s (MPa)	5.0	5.0	5.0	5.0	5.0	5.0	5.0	5.0
E_pI_p/E_sI_s	30	84	200	440	640	2000	6000	13800

[*] Additional model-scale pipes used in the parametric study.
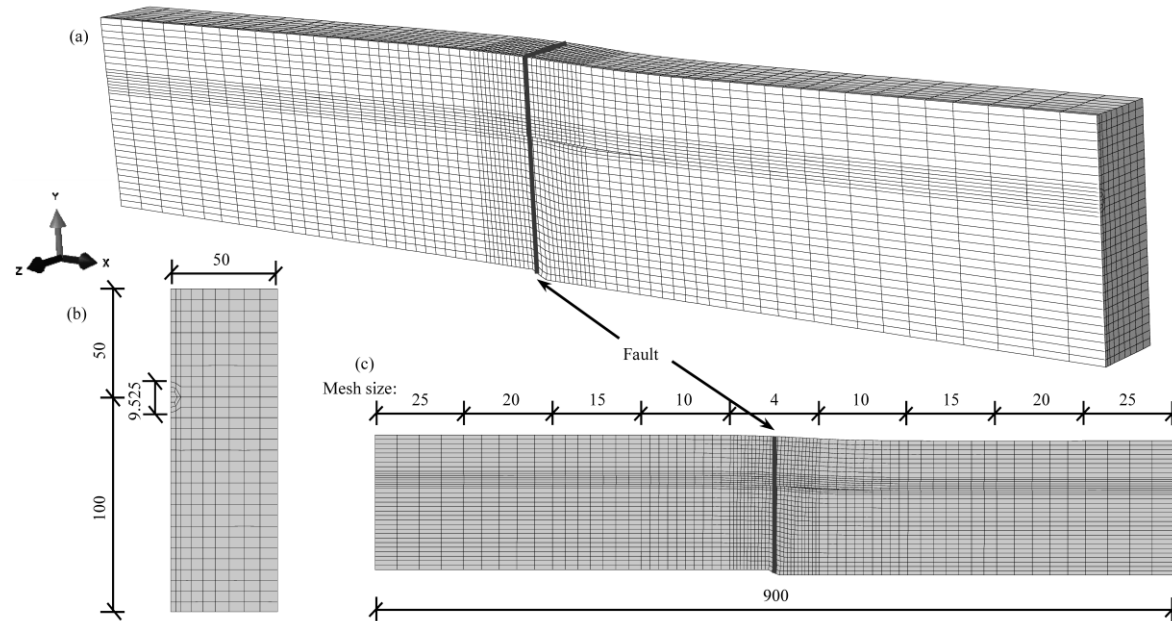
Figure 3. Finite element discretization of the (a) soil formation with tectonic fault, (b) cross-section and (c) elevation view

3   FINITE ELEMENT SIMULATION

Numerical modeling is performed using Dynamic/Explicit mode in the general-purpose finite element code ABAQUS (Hibbitt et al. 2001). The finite element mesh discretization presumed for the analysis is portrayed in Figure 3. Finite element size should correspond to 10 to 18.5 times the mean grain size to model the shear localization within soils (Muir Wood, 2002). To be consistent with the fault-foundation interaction studies (Anastasopoulos et al. 2007; Loli et al. 2012), the mesh size is calculated to be 4 mm based on the typical estimation of $16d_{50}$ near the fault. A coarser mesh is used at the pipe ends. The model width is reduced from 300 mm to 50 mm to accelerate the analysis, since the boundary effect can be minimized once the distance from the pipe to the boundary is 5 times larger than the pipe diameter (Vazouras et al. 2010).

The pipe is modeled as a half solid rod against a symmetric smooth rigid wall. Linear elastic properties are assigned as tabulated in Table 1, along with four additional relative pipe-soil stiffnesses to provide a more complete range of relative stiffness in the parametric study. The surrounding soil is characterized using the Mohr-Coulomb model. Strain softening was not modeled (Robert 2010; Trautmann 1983; Yimsiri et al. 2004). This modeling strategy reduces the computational effort; more sophisticated modeling may be undertaken in the future.

Fault propagation through the soil layer is normally regarded as a quasi-static process even during earthquakes. Hence, all soil parameters are determined from drained triaxial tests on the Fraser River sand (Karimian 2006). A constant volume internal friction angle (φ_{cv}) of 34° is used to estimate the response of the sand (Vaid et al. 2001). Secant modulus (E_{sec}), peak friction angle (φ_p) and dilation angle (ψ) that vary with depth are implemented. Table 2 shows the constitutive parameters for the soil used in the numerical model and a set of average representative properties reported by Saiyar (2011) for the soil above the pipe. A contact surface model is adopted that captures finite sliding and/or separation between the pipe and the soil. The influence of the interface friction coefficient on the flexural response of the pipe is negligible (Vazouras et al. 2012). Therefore, a constant value of 0.3 is employed, equivalent to 2/3 of the soil friction angle (Yimsiri et al. 2004).

Modeling of the fault across a narrow zone using a ramp function with width r can overcome numerical difficulties that may arise when modeling a sudden dislocation of elements at the fault. The fault offset varies linearly from zero at the footwall side to a maximum at the hanging wall side. A sensitivity study with respect to the width r shows that three times the element size ($3d_{FE}$), 12 mm, is optimal to avoid numerical errors and represent the correct ground motion.

4 NUMERICAL RESULTS

4.1 Free Field Soil Response

Shear strain localizes progressively within the soil overlying a fault depending on the physical restraint associated with the soil stiffness and the bedding depth *BD*. The dependence of the displacement discontinuity on depth can be seen in the free field test undertaken without a model pipe. The displacements measured in the centrifuge test are compared with those obtained from the numerical modeling in Figure 4. An intensive displacement gradient develops at the shear zone, and this region of high gradient shows the orientation of the shear zone. Large soil distortions can be expected near the base rock. A wider distributed displacement discontinuity develops where the fault approaches the ground surface.

Table 2. Soil parameters for Mohr-Coulomb modeling in ABAQUS (soil depth given in prototype scale).

Soil layer	Depth from surface (m)	Depth at center (m)	Confining stress (kPa)	Density (kN/m^3)	Poisson's ratio	φ_p (°)	φ_{cv} (°)	ψ (°)	c (kPa)
1	0.0-0.6	0.3	2	1610	0.3	48.6	34	29.1	3
2	0.6-1.2	0.9	6	1610	0.3	47.8	34	27.6	3
3	1.2-1.8	1.5	11	1610	0.3	47.1	34	26.1	3
4	1.8-2.4	2.1	15	1610	0.3	46.4	34	24.9	3
5	2.4-3.0	2.7	19	1610	0.3	45.9	34	23.8	3
6	3.0-3.6	3.3	24	1610	0.3	45.4	34	22.8	3
7	3.6-4.5	3.75	27	1610	0.3	45.1	34	22.2	3
Rep[*]				1610	0.3	48.2	34	28.4	3

[*] Representative uniform soil property above pipe burial depth.
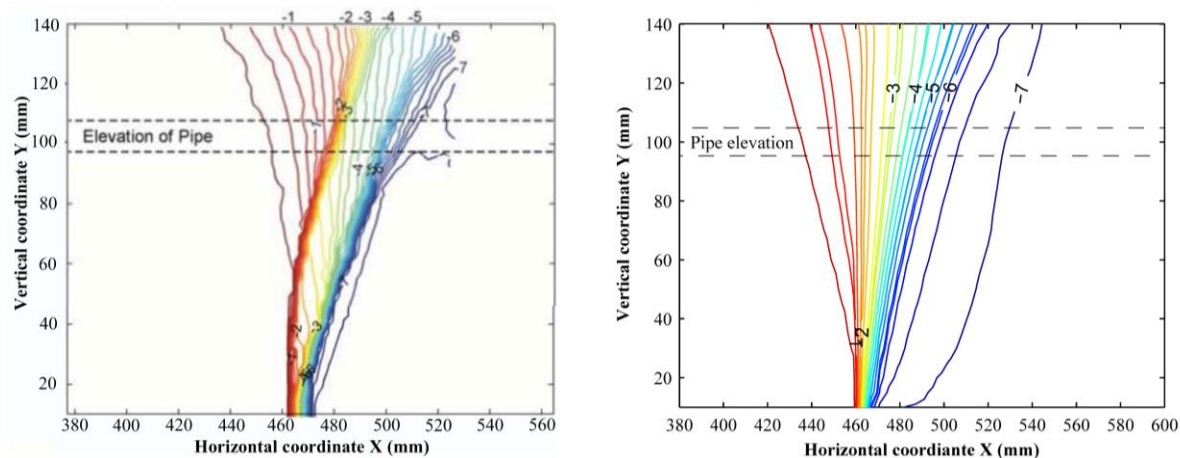
Figure 4. Free field soil response: vertical displacements in centrifuge test (left) and numerical analysis (right)

4.2 Flexural Response of Pipe

Figure 5 provides a comparison of displacement contours for the Aluminum model pipe obtained from the centrifuge test and the finite element analysis. The stiff pipe alters fault propagation through the soil, with spreading of the fault rupture along the pipe which bridges across the shear zone. A more inclined shear band is formed in the soil under the pipe, which induces a shift in the point of contraflexure towards the hanging wall. At the same time, the displacement discontinuity is more widely distributed above the pipe. The fault rupture appears to prefer an easier propagation path that avoids the high stiffness pipe structure within the soil layer. Diversion of the rupture zone has also been reported in fault-foundation interaction studies (Anastasopoulos et al. 2009; Loli et al. 2011). The larger the pipe stiffness, the wider the shear zone produced.

The curvature distribution along the pipe length can be derived from the deflection profile using the thin beam assumption. Figure 6 shows that the numerical method is capable of reproducing the flexural responses of the Aluminum pipe captured in the centrifuge test. Non-symmetric responses are observed, where a slightly larger curvature is computed in the footwall side (the hogging zone) than the hanging wall side (the sagging zone). Pipe hogging deflection is resisted by bearing capacity under the pipe, while the resistance in the sagging zone is governed by the uplift capacity of the overlying soil. These two mechanisms lead to different curvature distribution since the bearing capacity is larger than its uplift counterpart. As the second derivative is employed, errors inevitably arise in the curvature calculation. Overall, the finite element analyses provide reliable estimates of the flexural pipe responses (e.g., the difference in the peak curvatures calculated in the two analyses are within 8%).
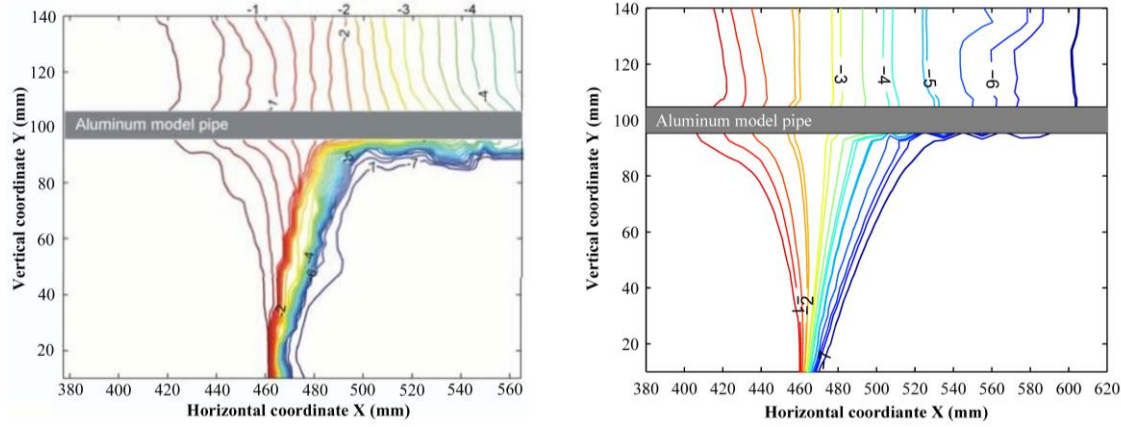
Figure 5. Pipe response: vertical displacements in centrifuge test (left) and numerical modeling (right)
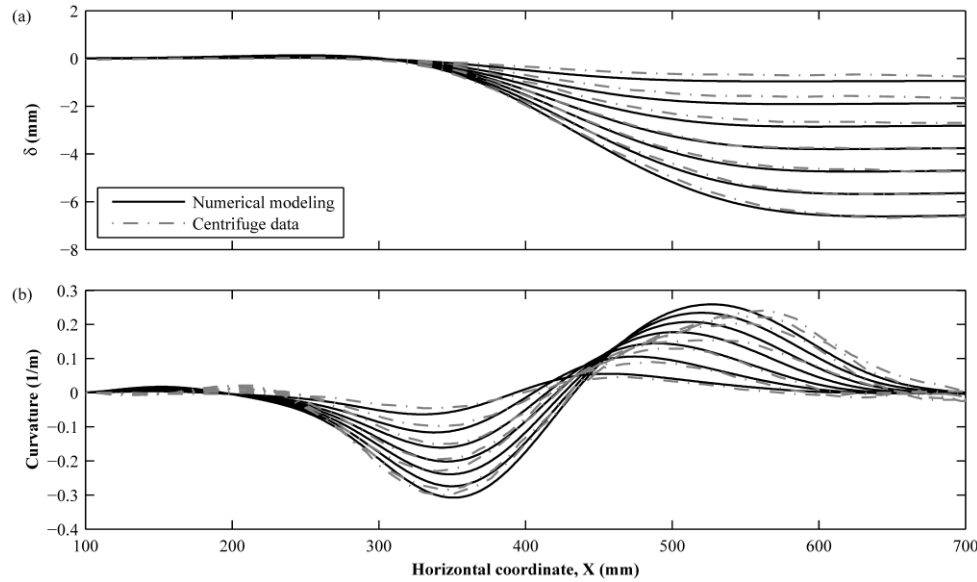
Figure 6. Aluminum pipe response: (a) deflections and (b) curvatures

4.3 Approximate Design Equations

The soil deformation pattern is often approximated as a continuous deformed line using a mathematical function. Effective estimates of the ground discontinuity experienced by the pipe is important for evaluation of pipe performance where it crosses ground faults. Saiyar (2011) defined the distance from the location of the point of contraflexure (x_c) to its peak curvature (κ_{max}) point as i_{soil} and i_{pipe} for the soil profile in the free field test and the pipe deflection in the pipe tests, respectively. She employed a modified error function as follows:

$$\delta(x) = \frac{1}{2}\delta_0\left(1 + erf\left(\frac{x - x_c}{\sqrt{2}i_{soil}}\right)\right) \qquad [1]$$

Assuming a flexible pipe has the same stiffness as the soil cylinder being replaced, double differentiation and rearrangement of the error function gives peak curvature occurring at $x\text{-}x_c = i_{pipe}$, normalized using fault offset δ_0:

$$\left|\frac{\kappa_{max}i_{pipe}^2}{\delta_0}\right| = \frac{1}{\sqrt{2\pi}}e^{-\left(\frac{1}{\sqrt{2}}\right)^2} = 0.24 \qquad [2]$$

A mean i_{soil} value of about 21.3 mm is obtained using the error function to interpret the finite element analysis results. In the centrifuge test, i_{soil} is inferred to have an average value of 17 mm (Saiyar 2011). To improve the accuracy of the calculation in the numerical modeling, a modified generalised logistic function is proposed for approximation of the free field soil response.

$$\delta(x) = -\frac{\delta_0}{\left(1 + \nu e^{-\left(c\frac{x - x_c}{i_{soil}}\right)}\right)^{1/\nu}} \qquad [3]$$

$$C = \ln\left(\frac{v}{2} + \frac{\sqrt{v^2 + 6v + 5}}{2} + \frac{3}{2}\right) \quad [4]$$

$$\left|\frac{\kappa_{max} i_{pipe}^2}{\delta_0}\right| = C^2 e^{-C}\left(ve^{-C} + 1\right)^{-(1/v+1)}$$

$$-C^2(v+1)e^{-2C}\left(ve^{-C}+1\right)^{-(1/v+2)} = 0.167 \quad [5]$$

where, the coefficient v of 0.8 is used to produce curvatures that are non-symmetric about the point of contraflexure.

A better evaluation of i_{soil} is achieved when the numerical modeling is interpreted using the logistic function, with average i_{soil} value of 16.6 mm (close to the value of 17 mm obtained in the test).

The lower bound of the normalized peak curvature corresponds to the case when the flexible pipe has stiffness equivalent to the soil replaced. The error and logistic functions give values of 0.242 and 0.167, respectively. A pipe constrained at both ends, corresponding to a beam with both fixed boundary conditions, provides an upper bound estimate. Classical beam theory provides normalized curvature of 1.5. In reality, the pipe stiffness and the anchorage condition should be between the flexural resistances provided by both the lower and the upper bounds.

Given the success of the finite element analyses of the centrifuge tests, a short parametric study (Table 1)

helps to extend the database with various pipe properties. Incorporating both the centrifuge and numerical data, Figure 7 exhibits the correlation between the i_{pipe}/i_{soil} ratio and the relative pipe-soil stiffness, along with a linear approximation:

$$\frac{i_{pipe}}{i_{soil}} = m \cdot \ln\left(\frac{E_p I_p}{E_s I_s}\right) + n \quad [6]$$

where, the non-dimensional parameters m and n are determined to be 0.56 and -0.66. When the deflection of the flexible pipe is in phase with the soil response, it produces a lower bound i_{pipe}/i_{soil} ratio of 1, corresponding to the relative pipe-soil stiffness of 20. To minimize the associated fitting errors, the lower bound of relative pipe-soil stiffness is conservatively estimated as 30, which conforms to PVC pipe backfilled by medium stiffness clay or HDPE pipe buried in very soft clay. A notable dispersion of the i_{pipe}/i_{soil} ratio for stiff pipe (curvature varies significantly at the right hand side of Figure 7) is a sign of the change of the soil-structure interaction mechanism. The thin beam theory is then no longer appropriate for use in deriving the curvature distributions and the proposed approach is not valid. Therefore, an upper bound of relative pipe-soil stiffness is chosen arbitrarily as 10,000, corresponding to the rigid pipe, such as cast and ductile iron and steel pipe, buried in backfill materials other than very soft clay.
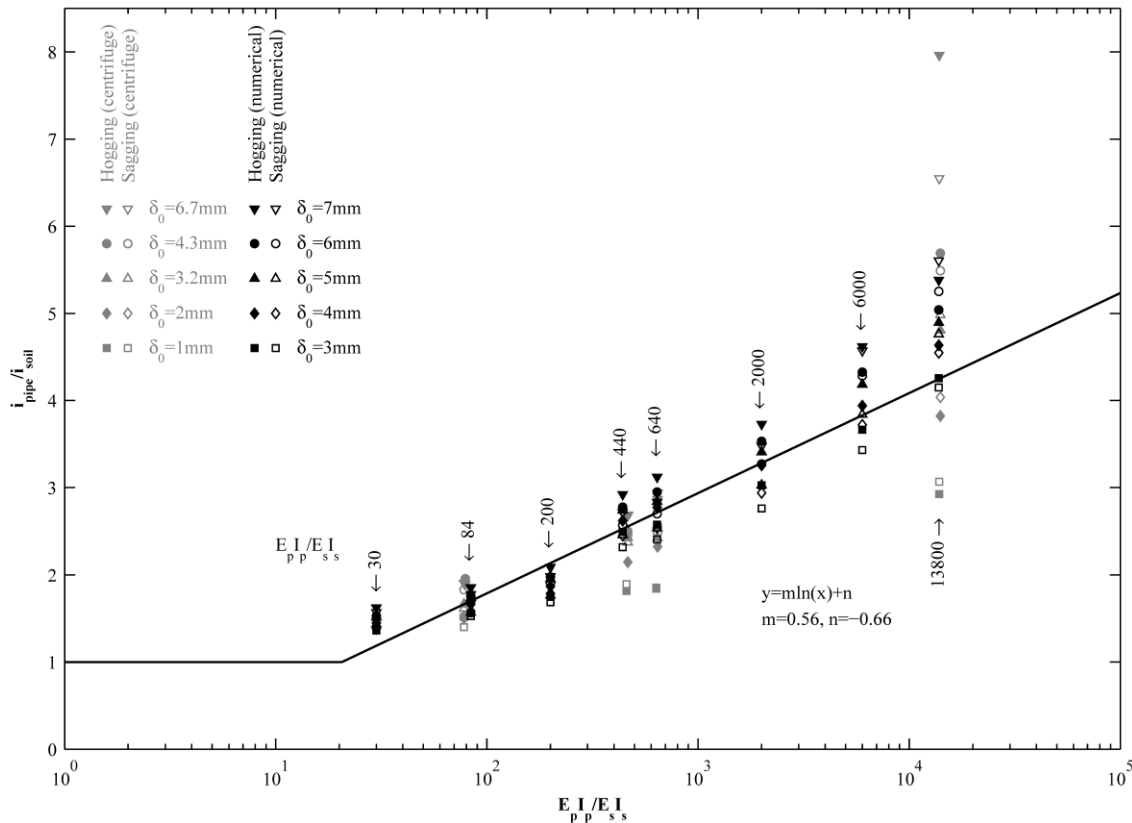
Figure 7. Ratio of i_{pipe}/i_{soil} varying with the relative pipe-soil stiffness

The normalized peak curvatures obtained from both the centrifuge tests (Ha et al. 2008; Saiyar 2011) and the finite element modeling are plotted in Figure 8. The logistic function provides a lower bound that is superior to the value achieved using the error function. As a first approximation, Saiyar (2011) suggested use of normalized peak curvature of 0.28. However, it can be seen that this constant value is lower than most of the results. In order to better interpret the data, the 84th and 16th percentiles are being proposed here using the least squares method by adding or subtracting one standard deviation from the mean (50th percentile) of all data. The peak curvature is larger in the pipe hogging deflection zone (Ni et al. 2014), and the 84th percentile envelope for the hogging data is suggested for use in design.
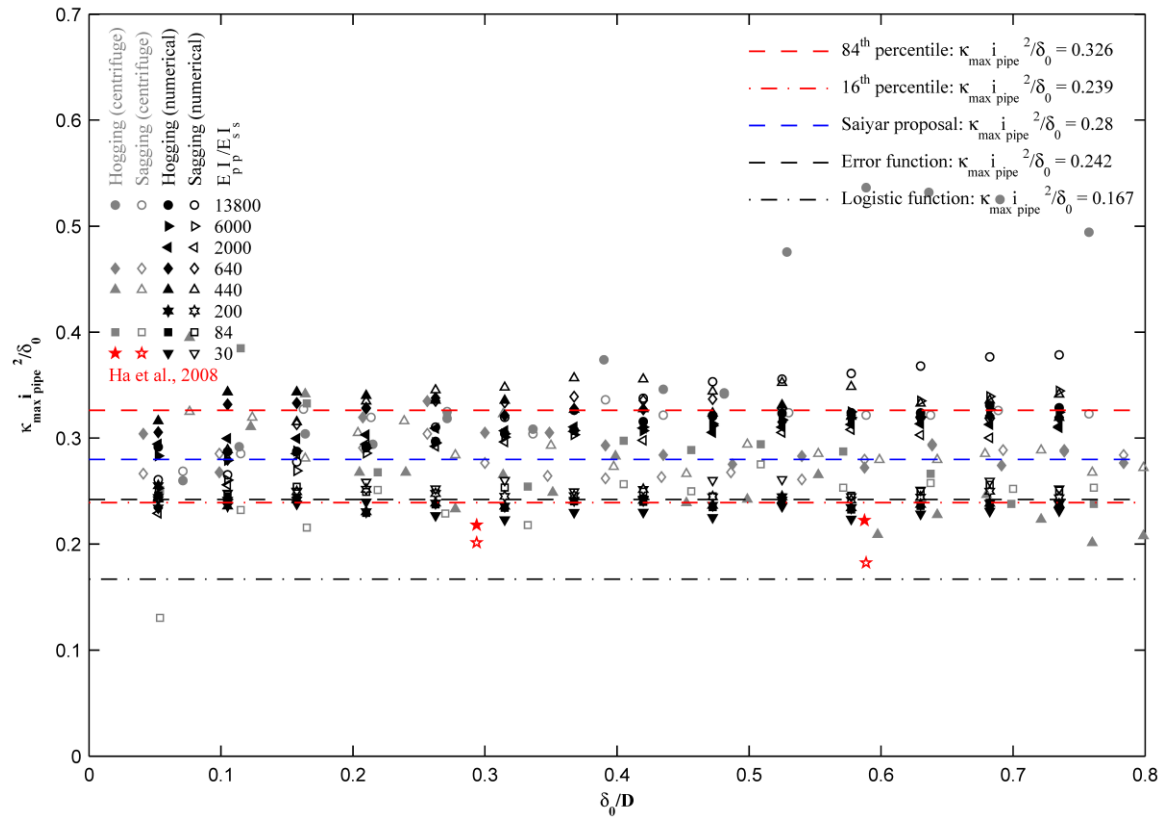
Figure 8. Normalized peak curvatures as a function of fault offset and pipes of different relative stiffness

5   CONCLUSIONS

This paper investigates the detrimental effect of a normal fault on the flexural response of a buried pipe which passes across it. Reduced-scale centrifuge tests are used to benchmark a three dimensional finite element model. A short parametric study provides data for a range of pipe stiffness values, using both the centrifuge and finite element modeling, and this information was used to develop approximate design equations to serve as a first approximation for the peak longitudinal bending moments during design.

Free field soil response can be expressed by either modified error or generalised logistic function. The distance from the location of the point of contraflexure (at or near the concentrated shear zone that develops in the soil) and the point of peak curvature is denoted as i_{soil}. A linearized fitting function is proposed for use in estimating i_{pipe}. The normalized peak pipe curvature can then be easily evaluated based on a given fault level. Bending strains or moments are directly related to the curvature, which can indicate the selection of design parameters.

The new design framework has the following limitations: (a) it is only applicable to continuous pipe intersecting at 90° a normal fault with dip angle of 90° (b) dense sand is used as backfill; (c) pipe is loaded in the elastic range; (d) relative pipe-soil stiffness varies from 30 to 10,000; (e) geometry is limited to pipe burial depth of 1.5 m, bedding depth of 3 m (bedding thickness to the rock below the pipe), and pipe diameter of 285 mm. Work is underway to extend the method to analyze other soil types and project geometries and to evaluate the design framework using large-scale geotechnical testing.

REFERENCES

Anastasopoulos, I., Gazetas, G., Bransby, M.F., Davies, M.C.R., and El Nahas, A. 2007. Fault rupture propagation through sand: finite-element analysis and validation through centrifuge experiments. *Journal of Geotechnical and Geoenvironmental Engineering* 133(8): 943-958.

Anastasopoulos, I., Gazetas, G., Bransby, M.F., Davies, M.C.R., and El Nahas, A. 2009. Normal fault rupture interaction with strip foundations. *Journal of Geotechnical and Geoenvironmental Engineering* 135(3): 359-370.

ASCE. 1984. *Guidelines for the seismic design of oil and gas pipeline systems*. American Society of Civil Engineers, Committee on Gas Liquid Fuel Lifelines.

Ha, D., Abdoun, T.H., O'Rourke, M.J., Symans, M.D., O'Rourke, T.D., Palmer, M.C., and Stewart, H.E. 2008. Buried high-density polyethylene pipelines subjected to normal and strike-slip faulting - a centrifuge investigation. *Canadian Geotechnical Journal* 45(12): 1733-1742.

Hibbitt, Karlsson, and Sorensen. 2001. *ABAQUS/Explicit: User's Manual (Vol. 1)*, Hibbitt, Karlsson and Sorenson Incorporated.

Karamitros, D.K., Bouckovalas, G.D., and Kouretzis, G.P. 2007. Stress analysis of buried steel pipelines at strike-slip fault crossings. *Soil Dynamics and Earthquake Engineering* 27(3): 200-211.

Karamitros, D.K., Bouckovalas, G.D., Kouretzis, G.P., and Gkesouli, V. 2011. An analytical method for strength verification of buried steel pipelines at normal fault crossings. *Soil Dynamics and Earthquake Engineering* 31(11): 1452-1464.

Karimian, S.A. 2006. *Response of buried steel pipelines subjected to longitudinal and transverse ground movement*. Ph.D. thesis, Department of Civil Engineering, The University of British Columbia, Vancouver, B.C.

Kennedy, R.P., Chow, A., and Williamson, R. 1977. Fault movement effects on buried oil pipeline. *Journal of Transportation Engineering* 103(5): 617-633.

Loli, M., Anastasopoulos, I., Bransby, M.F., Ahmed, W., and Gazetas, G. 2011. Caisson foundations subjected to reverse fault rupture: centrifuge testing and numerical analysis. *Journal of Geotechnical and Geoenvironmental Engineering* 137(10): 914-925.

Loli, M., Bransby, M.F., Anastasopoulos, I., and Gazetas, G. 2012. Interaction of caisson foundations with a seismically rupturing normal fault: centrifuge testing versus numerical simulation. *Geotechnique* 62(1): 29-43.

Muir Wood, D. 2002. Some observations of volumetric instabilities in soils. *International journal of solids and structures* 39(13): 3429-3449.

Newmark, N.M., and Hall, W.J. 1975. Pipeline design to resist large fault displacement. *U.S. National Conference on Earthquake Engineering*, Ann Arbor, MI.

Ni, P., Moore, I.D., and Take, W.A. 2014. The interaction of normal faults with pipelines: experimental observation and finite element modeling. *Annual Conference of the Canadian Society for Civil Engineering 2014: Sustainable Municipalities, CSCE 2014*, Halifax, NS.

O'Rourke, M.J., and Liu, X. 1999. *Response of buried pipelines subject to earthquake effects*. Monograph No. 3, Multidisciplinary Center for Earthquake Engineering Research, University at Buffalo.

Robert, D.J. 2010. *Soil-pipeline interaction in unsaturated soils*. Ph.D. thesis, University of Cambridge, UK.

Saiyar, M. 2011. *Behaviour of buried pipelines subject to normal faulting*. Ph.D. thesis, Queen's University, Kingston, ON, Canada.

Saiyar, M., Take, W., and Moore, I. 2011. Validation of boundary PIV measurements of soil–pipe interaction. *International Journal of Physical Modelling in Geotechnics* 11(1): 23-32.

Schofield, A.N. 1980. Cambridge geotechnical centrifuge operations. *Geotechnique* 30(3): 227-268.

Taylor, R.N. 2004. *Geotechnical Centrifuge Technology*. Taylor & Francis.

Trautmann, C.H. 1983. *Behavior of pipe in dry sand under lateral and uplift loading*. In Other Information: Thesis (Ph. D.). p. Medium: X; Size: Pages: 328.

Trifonov, O.V., and Cherniy, V.P. 2010. A semi-analytical approach to a nonlinear stress strain analysis of buried steel pipelines crossing active faults. *Soil Dynamics and Earthquake Engineering* 30(11): 1298-1308.

Vaid, Y.P., Stedman, J.D., and Sivathayalan, S. 2001. Confining stress and static shear effects in cyclic liquefaction. *Canadian Geotechnical Journal* 38(3): 580-591.

Vazouras, P., Karamanos, S.A., and Dakoulas, P. 2010. Finite element analysis of buried steel pipelines under strike-slip fault displacements. *Soil Dynamics and Earthquake Engineering* 30(11): 1361-1376.

Vazouras, P., Karamanos, S.A., and Dakoulas, P. 2012. Mechanical behavior of buried steel pipes crossing active strike-slip faults. *Soil Dynamics and Earthquake Engineering* 41: 164-180.

Wang, L.R.L., and Yeh, Y.H. 1985. A refined seismic analysis and design of buried pipeline for fault movement. *Earthquake Engineering & Structural Dynamics* 13(1): 75-96.

Wijewickreme, D., Sriskandakumar, S., and Byrne, P. 2005. Cyclic loading response of loose air-pluviated Fraser River sand for validation of numerical models simulating centrifuge tests. *Canadian geotechnical journal* 42(2): 550-561.

Yimsiri, S., Soga, K., Yoshizaki, K., Dasari, G.R., and O'Rourke, T.D. 2004. Lateral and upward soil-pipeline interactions in sand for deep embedment conditions. *Journal of Geotechnical and Geoenvironmental Engineering* 130(8): 830-842.